



Analysis of structural and magnetic phase transition behaviors of $\text{La}_{1-x}\text{Sr}_x\text{CrO}_3$ by measurement of heat capacity with thermal relaxation technique

Yuhta Matsunaga^a, Hitoshi Kawaji^b, Tooru Atake^b, Hiroki Takahashi^c, Takuya Hashimoto^{a,*}

^a Department of Integrated Sciences in Physics and Biology, College of Humanities and Sciences, Nihon University, 3-25-40 Sakurajousui, Setagaya-ku, Tokyo 156-8550, Japan

^b Materials and Structures Laboratory, Tokyo Institute of Technology, 4259 Nagatsuta, Midori-ku, Yokohama 226-8503, Japan

^c Department of Physics, College of Humanities and Sciences, Nihon University, 3-25-40 Sakurajousui, Setagaya-ku, Tokyo 156-8550, Japan

ARTICLE INFO

Article history:

Received 11 March 2008

Received in revised form 22 May 2008

Accepted 5 June 2008

Available online 14 June 2008

Keywords:

$\text{La}_{1-x}\text{Sr}_x\text{CrO}_3$

Heat capacity

Structural phase transition

Magnetic phase transition

Crystal structure

ABSTRACT

The heat capacity, C_p , of the $\text{La}_{1-x}\text{Sr}_x\text{CrO}_3$ system and its temperature dependence have been measured by a thermal relaxation technique. Both structural and magnetic phase transitions were detected at temperatures that can be surmised from the phase diagram proposed in previous studies. The observed variation in enthalpy after the first-order structural phase transition, ΔH , showed agreement with those measured by differential scanning calorimetry (DSC). A decrease in the variation in C_p in the second-order magnetic phase transition, ΔC_p , with an increase in Sr content was detected, which can be attributed to a decrease in electronic spin configuration entropy with an increase in Sr content. In the dependence of ΔC_p on Sr content, a bending point was also observed at $x \sim 0.12$, at which the crystal system varies from an orthorhombic-distorted perovskite structure to a rhombohedral-distorted perovskite structure.

© 2008 Elsevier B.V. All rights reserved.

1. Introduction

Oxides with a perovskite-type crystal structure including a 3d transition metal, $\text{La}_{1-x}\text{Ae}_x\text{MO}_3$ (Ae = Ca, Sr; M: 3d transition metal) show interesting property such as a high electrical conductivity at high temperatures in various gas atmospheres and a colossal magnetic resistance (CMR) [1–3]. The magnetic, electric and thermodynamic properties of $\text{La}_{1-x}\text{Ae}_x\text{MO}_3$ are affected by a slight distortion from the ideal cubic perovskite structure, which is often observed in most perovskite-type oxides. Therefore, clarifying the relationship between the precise crystal structure and the above-mentioned properties is essential for practical applications; however, the authors consider that there have been few exhaustive reports since oxygen non-stoichiometry, which should generate under some preparation conditions and is a factor affecting the crystal structure and properties, was not considered in most studies.

Among $\text{La}_{1-x}\text{Ae}_x\text{MO}_3$, $\text{La}_{1-x}\text{Ae}_x\text{CrO}_3$ prepared in O_2 or air is reported to have no oxygen deficiency regardless of Ae content, as determined from the results of thermogravimetry [4–6]. Thus, we regard that $\text{La}_{1-x}\text{Ae}_x\text{CrO}_3$ is the most suitable material for analyzing the relationship between crystal structure and various

properties since distortion from the ideal cubic perovskite structure and chemical state of Cr, *i.e.*, the concentrations of holes and spins are determined only by Ae content. Moreover, the origin of the magnetic property of $\text{La}_{1-x}\text{Ae}_x\text{CrO}_3$ is the super-exchange interaction of magnetic spin on the t_{2g} orbital of the B site Cr ion. Because a similar super-exchange interaction of magnetic spin on an e_g orbital is proposed for $\text{La}_{1-x}\text{Ae}_x\text{MnO}_3$, which has been extensively studied as CMR materials, particularly at low Ae content, the analysis of the relationship between the crystal structure and magnetic property of $\text{La}_{1-x}\text{Ae}_x\text{CrO}_3$ might be the first step in elucidating the CMR mechanism of $\text{La}_{1-x}\text{Ae}_x\text{MnO}_3$.

In our previous study [7], we have analyzed the structural and magnetic phase transition of $\text{La}_{1-x}\text{Sr}_x\text{CrO}_3$ by differential scanning calorimetry (DSC), dilatometry, temperature-controlled X-ray diffraction analysis, and dc magnetic measurement using SQUID. Two types of phase transition, namely first-order structural phase transition from orthorhombic-distorted perovskite to rhombohedral-distorted perovskite and second-order phase transition from canted antiferromagnetic to paramagnetic, were observed. Phase transition temperature changed with Sr content, and we proposed a magnetic and structural phase diagram of $\text{La}_{1-x}\text{Sr}_x\text{CrO}_3$, which includes four phases: paramagnetic-orthorhombic, canted antiferromagnetic-orthorhombic, canted antiferromagnetic-rhombohedral, and paramagnetic-rhombohedral. In particular, we have measured the dependence of magnetization on external magnetic field at

* Corresponding author. Tel.: +81 3 3329 1151x5516; fax: +81 3 5317 9432.

E-mail address: takuya@chs.nihon-u.ac.jp (T. Hashimoto).

various temperatures for specimens with an Sr content x higher than 0.12 [8]. It has been revealed that the residual magnetization and coercive force of canted antiferromagnetic phase are affected by the first-order structural phase transition.

According to the phase diagram previously proposed [7], two types of second-order phase transition from a canted antiferromagnetic phase to a paramagnetic phase are shown: one is observed in the phase of orthorhombic-distorted perovskite for specimens with x lower than 0.12, whereas the other is detected in rhombohedral-distorted perovskite for specimens with x higher than 0.12. It is probable that behavior of the second-order phase transition varies depending on crystal structure. However, even the direct measurement of heat capacity (C_p), the most fundamental thermodynamic property, has not been carried out for $\text{La}_{1-x}\text{Sr}_x\text{CrO}_3$ and its variation in the second-order phase transition, ΔC_p , has not been sufficiently estimated.

In this study, the C_p of $\text{La}_{1-x}\text{Sr}_x\text{CrO}_3$ below room temperature has been measured using a thermal relaxation technique. The evaluated C_p and observed phase transition behavior have been compared with the results observed by DSC and dc magnetic measurement. The effect of the crystal system on ΔC_p has been investigated for the first time.

2. Experimental

Polycrystalline specimens of $\text{La}_{1-x}\text{Sr}_x\text{CrO}_3$ ($x=0.00$ – 0.25) were prepared by the Pechini method [9]. Details of the preparation process are the same as those previously reported [7]. For powder X-ray diffraction analysis (Cu K α ; 50 kV, 250 mA, Rigaku RINT-2500) and differential scanning calorimetry (DSC; DSC8230, Rigaku Co., Ltd.), some of the obtained $\text{La}_{1-x}\text{Sr}_x\text{CrO}_3$ pellets were reground into powder in an alumina mortar. X-ray diffraction analysis at room temperature indicated that the obtained specimens were single-phase orthorhombic-distorted perovskite and rhombohedral one with $x < 0.10$ and $x > 0.10$, respectively. For $\text{La}_{0.9}\text{Sr}_{0.1}\text{CrO}_3$, a mixture of the two phases was obtained [10]. DSC was carried out by a method that is completely same as the previously reported one [7].

The dc magnetic susceptibility of the sintered $\text{La}_{1-x}\text{Sr}_x\text{CrO}_3$ was measured with a SQUID magnetometer (Quantum Design Inc., MPMS model). The temperature of the sample was controlled to be at measurement level after zero magnetic field cooling (ZFC) and then magnetic susceptibility was measured under an external magnetic field of 2 kOe. The measurement temperature range was 2.2–300 K at a heating rate of 1 K/min.

For C_p measurement, sintered $\text{La}_{1-x}\text{Sr}_x\text{CrO}_3$ pellets were shaped into rectangular form of about 2.0 mm \times 2.0 mm \times 1.0 mm. The C_p of the thus-shaped specimens were measured using PPMS (Physical Property measurement system; Quantum Design Inc.) with a heat capacity option by a thermal relaxation technique of the step scanning method under vacuum with a temperature range of 1.8–310 K.

3. Results

Fig. 1 shows the temperature dependence of the C_p of $\text{La}_{1-x}\text{Sr}_x\text{CrO}_3$. A heat capacity jump was observed for every $\text{La}_{1-x}\text{Sr}_x\text{CrO}_3$ as depicted by downward arrows. The temperature, at which the heat capacity jump was observed, decreased with an increase in Sr content. Fig. 2 shows the temperature dependence of the reciprocal of dc magnetic susceptibility, χ^{-1} , of $\text{La}_{1-x}\text{Sr}_x\text{CrO}_3$. A discrete increase in χ^{-1} was observed at temperatures depicted by upward arrows. Linear relationships were detected above the temperature as shown in dotted lines, indicating a paramagnetic

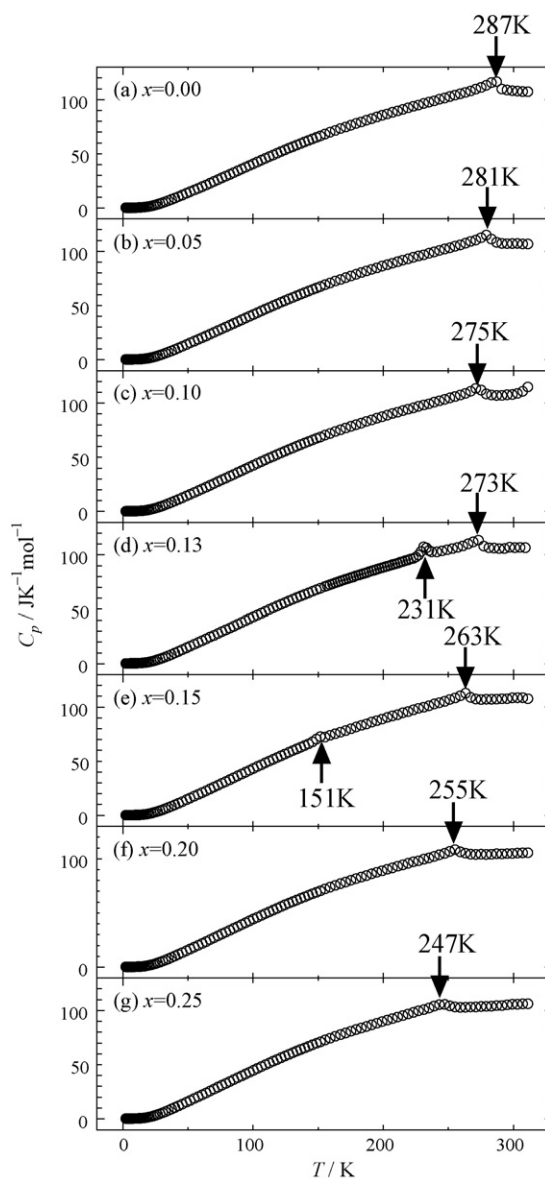


Fig. 1. Heat capacities of $\text{La}_{1-x}\text{Sr}_x\text{CrO}_3$: (a) $x=0.00$, (b) $x=0.05$, (c) $x=0.10$, (d) $x=0.13$, (e) $x=0.15$, (f) $x=0.20$, and (g) $x=0.25$ measured by thermal relaxation technique. Heat capacity jumps originating from the second-order magnetic phase transition are denoted by downward arrows. The peaks due to the first-order structural phase transition are represented by upward arrows.

property that obeys the Curie–Weiss law. The small χ^{-1} , *i.e.*, the large χ below the temperature suggested a canted antiferromagnetic property, which was confirmed from the dependence of magnetization on external magnetic field [7,8]. Since the temperatures denoted by upward arrows in Fig. 2 agreed, the heat capacity jump depicted by downward arrows in Fig. 1 can be ascribed to the second-order magnetic phase transition. This phase transition has also been detected in DSC curves as a baseline shift, as shown in Fig. 3 and Ref. [7]. A smaller baseline shift was observed with an increase in Sr content, showing correspondence with the smaller ΔC_p in the specimens with higher Sr content, which will be discussed later.

For the specimens with $x=0.13$ and 0.15 , additional peaks were detected at 231 K and 151 K, respectively, from the temperature dependence of C_p as shown in Fig. 1(d) and (e). These temper-

Download English Version:

<https://daneshyari.com/en/article/675405>

Download Persian Version:

<https://daneshyari.com/article/675405>

[Daneshyari.com](https://daneshyari.com)